

# Hemodynamic Characteristics of Dilated Ascending Aorta in Patients with Bicuspid Aortic Valve

Tie Zheng

Beijing An Zhen Hospital: Capital Medical University Affiliated Anzhen Hospital

Shijie Lu

Beijing An Zhen Hospital: Capital Medical University Affiliated Anzhen Hospital

Shuai Zhu

Beijing Luhe Hospital

Jiafu Ou

Washington University In St Louis: Washington University in St Louis

Jun-Ming Zhu ([✉ anzhenzjm@163.com](mailto:anzhenzjm@163.com))

Beijing An Zhen Hospital: Capital Medical University Affiliated Anzhen Hospital <https://orcid.org/0000-0002-6919-9164>

---

## Research

**Keywords:** Bicuspid aortic valve, Hemodynamics, Aortic dilatation, Aorta

**Posted Date:** November 16th, 2021

**DOI:** <https://doi.org/10.21203/rs.3.rs-940191/v1>

**License:**  This work is licensed under a Creative Commons Attribution 4.0 International License.

[Read Full License](#)

---

**Title: Hemodynamic characteristics of dilated ascending aorta in patients with bicuspid aortic valve**

Tie Zheng<sup>1</sup>, Shijie Lu<sup>1</sup>, Shuai Zhu<sup>2</sup>, Jiafu Ou<sup>3</sup>, Junming Zhu<sup>1\*</sup>

1 Department of Cardiovascular Surgery, Beijing Aortic Disease Center, Beijing Anzhen Hospital, Capital Medical University, Beijing, China; Beijing Institute of Heart Lung and Blood Vessel Diseases, Beijing 100029, China

2 Beijing Luhe Hospital, Capital Medical University, Beijing 101149, China;

3 Cardiology Division, Department of Internal Medicine, Washington University in St. Louis, 63110 USA

\*Corresponding authors:

Junming Zhu: anzhenjm@163.com

Fax: +86 10 64456595

## **Abstract**

**Objective:** Aim of this study is to investigate the influence of aortic diameter on hemodynamic environment characteristics in patient with the bicuspid aortic valve (BAV) and dilated ascending aorta (AAo) .

**Methods:** In this study, an MRI of one BAV patient with 4.5 cm AAo was collected and numerical model was constructed. Based on the images, the other three numerical models were constructed with different ascending aortic size with 4.0cm, 5.0cm and 5.5cm respectively while the size and the geometry of other parts were fixed. Then hemodynamics in these four models was simulated numerically and the flow patterns and loading distributions were investigated.

**Results:** Hemodynamics environments in the AAo were simulated with different aortic size. As the aortic diameter increases, we find: 1. the blood flow becomes more disturbing;2.the wall pressure at ascending aortic is higher; 3. the wall shear stress at the ascending aortic decreases; 4.oscillatory shear index of the outer part on the proximal AAo increases;5. all these hemodynamic parameters described above are asymmetrically distributed in dilated AAo and more parts of aorta would be affected as the AAo dilatation progresses.

**Conclusions:** The study revealed that the diameter of ascending aortic can significantly influence the magnitude and distribution of the dynamics. There are altered flow patterns, pressure difference, WSS and OSI distribution features in bicuspid aortic valve patients with vascular dilatation. As the extent of aortic dilatation increases especially exceed 5.5cm, this study support the recent guideline that aortic replacement should be considered .

**Key words:** **Bicuspid aortic valve, Hemodynamics, Aortic dilatation, Aorta**

## **Introduction**

The bicuspid aortic valve (BAV) is one of the common congenital heart anomalies in adults. BAV is an inherited form of heart disease in which two of the leaflets of the aortic valve fuse during embryonic development resulting in a two-leaflet valve (bicuspid valve) instead of the normal three-leaflet valve (trileaflet valve)<sup>1,2</sup>.

Previous studies have revealed two-leaflet valve will alter the physiological flow patterns in the ascending aorta (AAo), and the abnormal pulsatile flow patterns have effects on the endothelial cells of the arterial wall, then activate the remodeling process of artery wall, which cause the dilatation of AAo<sup>3,4,5</sup>. Therefore, the threshold for aortic repair is lower in aortopathy with BAV than normal. In 2020 ACC/AHA guideline, whether surgery is required in BAV mainly depends on the diameter of the AAo, especially in those diameters exceed 5.0 cm. And lifelong serial evaluation (MRI, CT, echocardiography) is reasonable in BAV with diameter of AAo exceed 4.0cm<sup>6</sup>.

Although many studies have proved the coincidence between BAV and the occurrence of ascending aortic dilatation<sup>7,8</sup>, few studies have focused on the hemodynamic environments in different diameter of AAo. We think that it is very vital to investigate and present the hemodynamic environments in different diameter of AAo for BAV patients. This study will help to discover the hemodynamic changes with the different diameters of AAo and provide further understanding of the aortic dilatation in patients with BAV.

## **Methods**

### **Patient**

This study was approved by local ethics committee (2016047X, Beijing Anzhen Hospital, Capital Medical University). This patient is 51 years old male, whose information was collected on August 3, 2016 in Anzhen hospital. He has BAV with left/right cusp fusion and mild-stenosis as well as dilated ascending aortic with diameter of 4.5 cm by echocardiography. We confirmed the patient doesn't have history of

hypertension, hyperlipidemia, coarctation of aorta, aortic dissection or Marfan syndrome.

### Numerical model of the aorta

The numerical model of the aorta was established based on the MRI data (in-plane resolution of 512 by 512 pixels with a pixel size of 0.7 mm and slice thickness of 1.25 mm, total 600 images). This MRI was obtained by the Trio Tim 3.0 T MRI scanner of Siemens of Germany, with the maximum switching rate of 200 T/(m · ms) and the maximum gradient strength of 45mt/m under the phase-controlled front ring and the electrocardiography gated control scan. Image segmentation and surface reconstruction of BAV were accomplished by a semi-automatic threshold-based segmentation tool (Mimics17.0, Materialise Inc., Belgium).

After smoothed, the format of aorta model was saved as X\_T format (a kind of parasolid model file format) from stereolithography by extracting surface function (Geomagic Wrap2015, Geomagic Inc., USA). Starting from the sinotubular junction to the end of AAo, aorta model was cut off in the maximum diameter. The profile of the cross-section at the maximum diameter of the AAo is traced, and the diameter of the cross-section was set to 4.0cm, 4.5cm, 5.0cm and 5.5cm, respectively. Along the aorta axis, lofting was made by contours of three sections by CAD (Computer Aided Design) tool (SolidWorks2015, SolidWorks Inc., France). The final four models named Model1, Model2, Model 3 and Model 4 (M1, M2, M3 and M4) are shown in **Fig.1**.

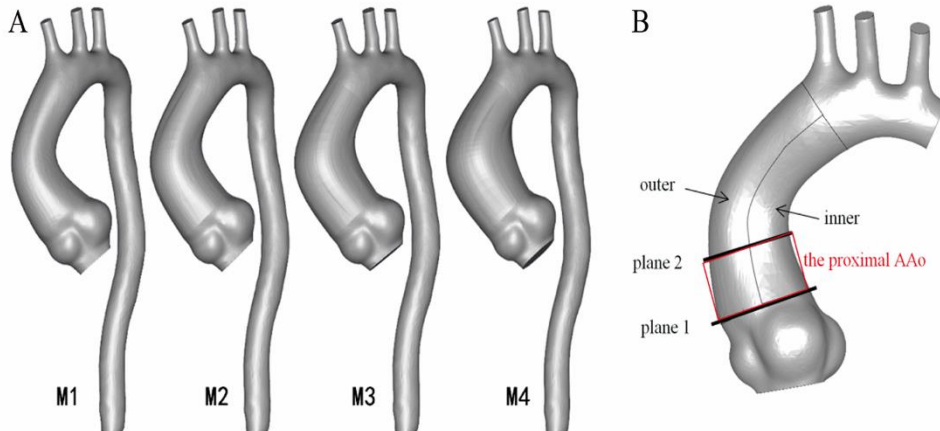


**Fig. 1**

Fig.1 Four numerical models of BAV numerical models were established. (A)The diameters of the ascending aorta (AAo) are 4.0cm, 4.5cm 5.0cm and 5.5cm, respectively; while, the size and the appearance of other parts are fixed; (B)Regions of interest where the hemodynamic were analyzed.

### Meshing

A semi-automatic adaptive meshing technique was employed in HyperMeshv10.0 (Altair HyperWorks, Troy, MI, USA) to optimize both computational efficiency and element quality. 4-noded tetrahedral elements were assigned to all models, and element size was set to 0.0014m and 5 boundary layers near the walls. The grid was divided into various entrance, exits and the inner/outer of AAo regions. The number of elements and nodes of models meshed are shown in **Table 1**.

	M1	M2	M3	M4
Elements	778406	822982	866242	915330
nodes	212904	222098	231944	241901

**Table 1** - The numbers of elements and nodes of each model

### Boundary conditions and flow models

Transient analysis was adopted to investigate the pulsatility of blood flow. No-slip boundary conditions were assigned at the wall in all cases. The numerical simulation

was based on the three-dimensional incompressible Navier-Stokes equations and continuity equations:

$$\rho \left[ \left( \frac{\partial \vec{u}}{\partial t} \right) + (\vec{u} \cdot \nabla) \vec{u} \right] + \nabla p - \nabla \cdot \tau = 0 \quad (1)$$

$$\nabla \cdot \vec{u} = 0 \quad (2)$$

Where  $\vec{u}$  and  $p$  represent the fluid velocity vector and the pressure respectively.  $\rho$  denotes the blood density ( $\rho = 1050 \text{ kg/m}^3$ ), and  $\tau$  is stress tensor. It was assumed that blood is incompressible, and blood has same kinematic viscosity and density of Newtonian fluid <sup>9,10</sup>.

Time-varying velocity profile was imposed at the inlet of the aorta, based on the flow velocity waveforms that had been obtained from the in vivo measurements. The flow rates entering the brachiocephalic, left common carotid, and left subclavian arteries were specified to be 12%, 5% and 8% of the blood flow rate entering the aortic root, respectively <sup>11,12</sup>.

The average Reynolds numbers ( $Re_{ave}$ ) based on the average flow velocity ( $V_{ave}$ ) at peak systole is 1149. The Womersley numbers( $\alpha$ ) is 22.5 and the blood flow is assumed to be laminar. The calculation time step and cardiac cycle were set to 0.01s and 0.8s, respectively. To minimize the influence of initial flow conditions, all simulations were carried out by a commercial finite-volume-based CFD solver (Fluent14.5, ANSYS, Inc., USA) for six cardiac cycles to achieve a periodic solution, and the results presented here were obtained in the sixth cycle.

### Derived Hemodynamic Parameters

Derived hemodynamic wall parameters include the velocity, pressure, WSS, and oscillatory shear index (OSI). WSS is an analytical factor used to describe the dynamic friction between the viscous fluid and the solid wall, which is caused by the lateral movement of the viscous fluid. The time-averaged wall shear stress (TAWSS) is obtained by averaging the WSS in a cardiac cycle and is a better representative of WSS.

$$TAWSS = \frac{1}{T} \int_0^T WSS dt \quad (3)$$

OSI reflects the cyclic departure of the WSS (or velocity) vector from predominant direction of blood flow and is calculated as equation (4):

$$OSI = \frac{1}{2} \left( 1 - \frac{\left| \int_0^T \tau_\omega dt \right|}{\int_0^T |\tau_\omega| dt} \right) \quad (4)$$

where  $\tau_\omega$  is wall shear stress and T is one cardiac cycle. The OSI values vary from 0 to 0.5: 0 represents unidirectional flow, and 0.5 signifies complete oscillatory flow.

In order to describe the results intuitively, five featured moments selected from one cardiac cycle based on the velocity waveform of the aortic inlet, including the early systolic phase ( $t=0.10s$ ), the peak systolic phase ( $t=0.17s$ ), the late systolic phase ( $t=0.29s$ ), the maximum regurgitation phase ( $t=0.43s$ ) and stable diastolic phase( $t=0.51s$ ), respectively. They were showed in **Fig.2**.

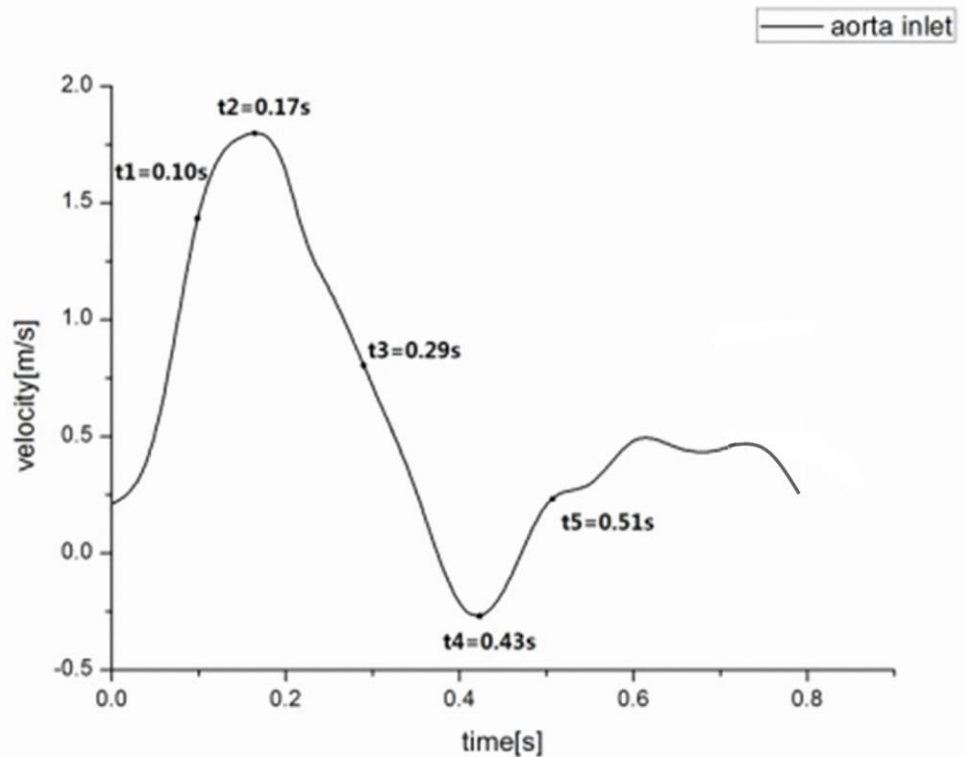


**Fig. 2**

Fig.2 The cross-sectional velocity profile of the inlet at the AAo. The data is obtained from in vivo measurements

## Results

### Flow velocity, patterns and ratio

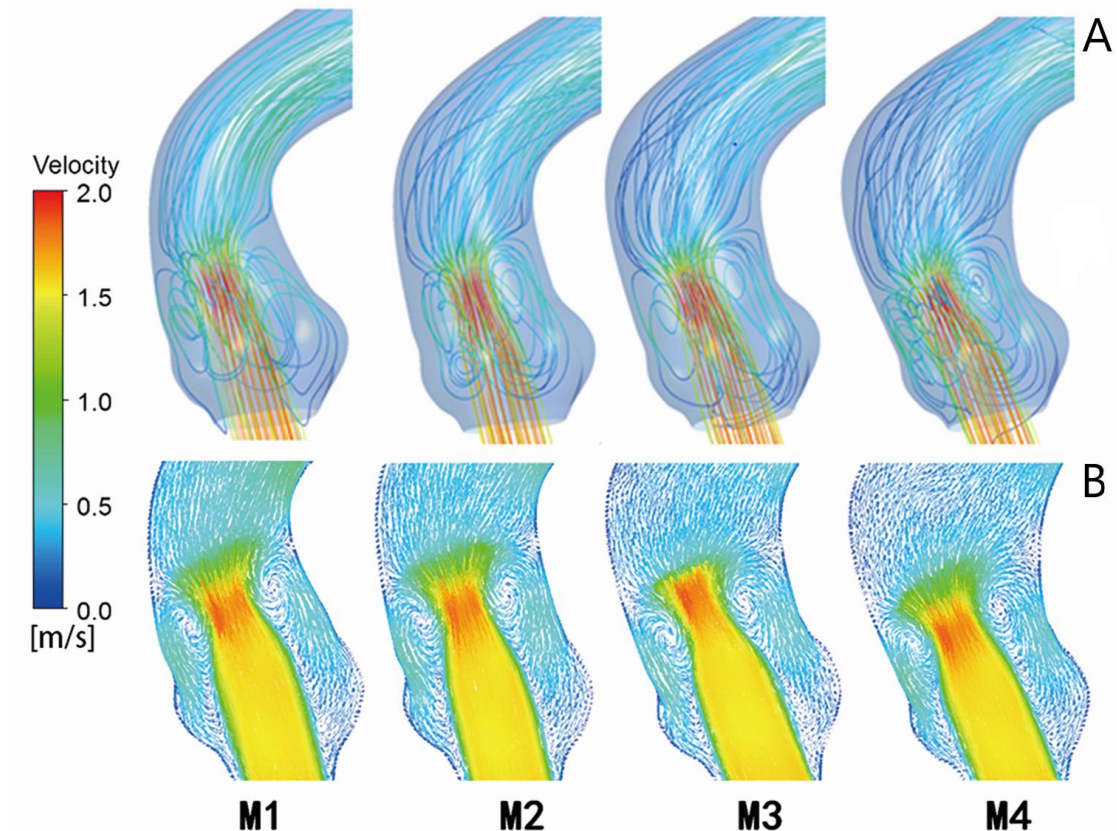


**Fig. 3**

Fig.3 Flow pattern within the AAo analysis at the peak systolic phase (A) and the late systolic phase (B) by drawing lines that are tangential to the instantaneous velocity vectors. These lines are contoured by velocity magnitude

Fig.3 shows the flow pattern within the aorta at the peak systolic phase and the late systolic phase. The aortic valve area is reduced by bicuspid aortic valve malformation, so when the blood flows into the aortic sinus at the peak systolic, the velocity is high, which is up to 2.2m/s. (The peak systolic velocity is high up tp 2.2 m/s due to mild stenosis of this BAV.) It was an important observation when compare this

velocity with the normal aortic entrance velocity (1.0-1.7m/s)<sup>13</sup>. However, the velocity of blood flow drops abruptly when flowing past the AAo and forms a large regurgitation, which makes more turbulent flow . At the late systolic phase, the turbulent blood flow rushes at the outer of the AAo wall. To observe the blood flow velocity better, the velocity profile of the sinotubular junction (plane 1) and the proximal AAo (plane 2) were analyzed, as shown in Fig.4a, 4b.

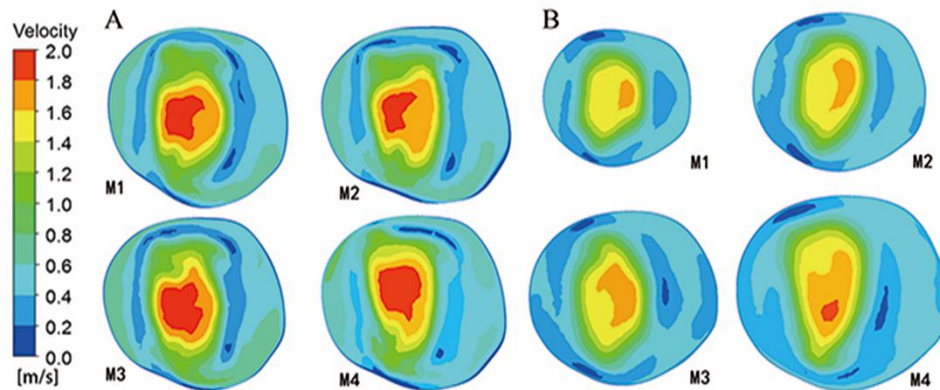


**Fig. 4**

Fig.4 Vector contours of two sections at peak systolic. The (A) and (B) display the flow pattern of the sinotubular junction (plane 1) and the proximal AAo (plane 2), respectively. The left side of contours is the outer and the right side is the inner

At peak systolic (Fig.4a at 0.17s), there is no significant difference in velocity among four models when the flow past the sinotubular junction. The velocity is higher in central blood flow and the flow velocity is lower near the wall of the vessel as expected. However, the velocity contours of the proximal AAo presented in Fig.4b at peak systolic are somewhat different: 1. the area with high velocity (velocity>1.6m/s, orange and red area) increased with the increasing diameter of the vessel; 2. when the AAo is dilated to the diameter of 5.5cm, the maximum velocity is obviously highest among models; 3. the area with high velocity is shifted to the left displaying a greater asymmetry with larger aorta.

## Pressure

The largest pressure difference (based on the ascending aortic inlet pressure) occurs at peak systolic, when blood flow velocity is the highest. The pressure difference from aortic annulus to AAo is depicted in Fig.5 . As the AAo diameter increases, the area of high pressure in AAo increases accordingly, especially in diameter is 5.5cm.

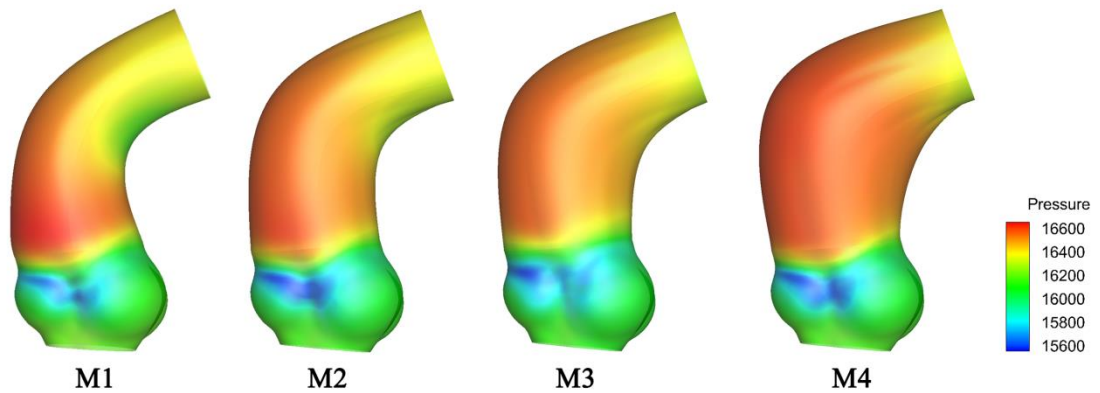


Fig.5 displays the WSS distributions of the four models with different diameters at peak systolic

### Wall shear stress distributions

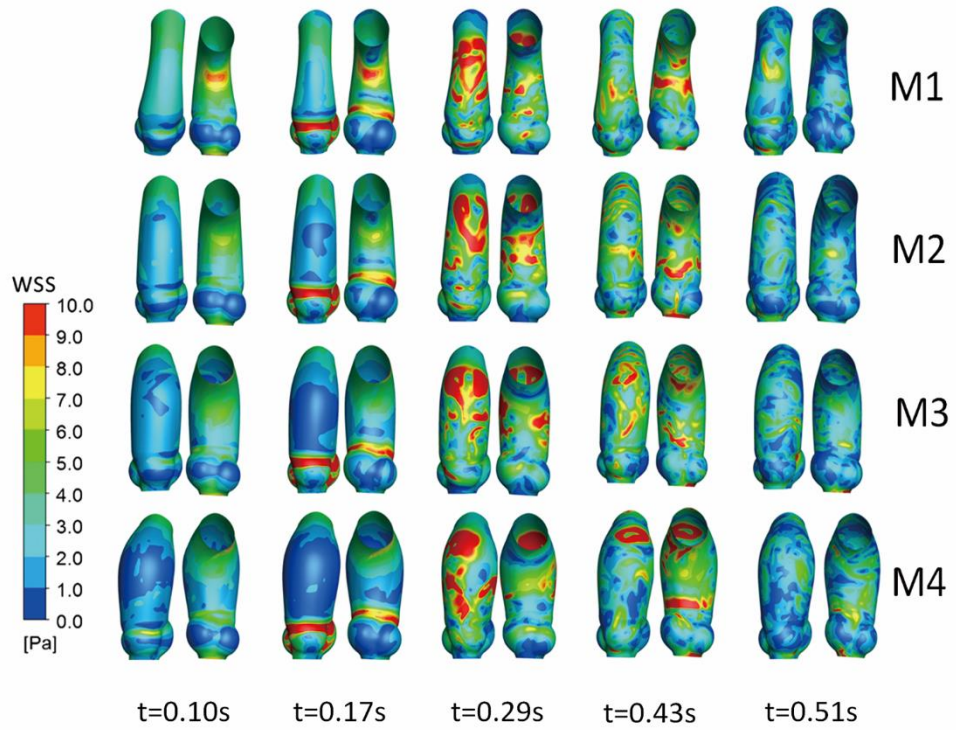


Fig. 6

Fig.6 displays the WSS distributions of the four models with different diameters at five feature moments

Fig. 6 displays wall shear stress contours at five featured moments. At peak systolic( $t=0.17s$ ), and flow is most furious when entering the valve, the proximal AAo wall shear stress(WSS) is much higher than that in other regions. As the diameter increases, the AAo has more area with low WSS.

The WSS distributions at the late systolic phase( $t=0.29s$ ) and the maximum regurgitation phase( $t=0.43s$ ) in all of the cases are above 10Pa around the mid-AAo, especially for the case with 5.5cm diameter. Additionally, at the late systolic phase( $t=0.29s$ ), the maximum WSS values of M1, M2, M3 and M4 are 24Pa, 27Pa, 28pa and 31Pa, respectively. At the early systolic phase( $t=0.10s$ ) and stable diastolic phase( $t=0.51s$ ), WSS values of the both sides are stable without obvious changes, for all cases.

### Oscillatory shear index

Fig. 7 shows when the AAo gets bigger, the area-averaged OSI of the outer part on the proximal AAo wall increases, while OSI of the inner part remains constant. Moreover, it is remarkable to see the OSI values of the outer exceeds that of the inner in M4 with aortic diameter of 5.5cm.

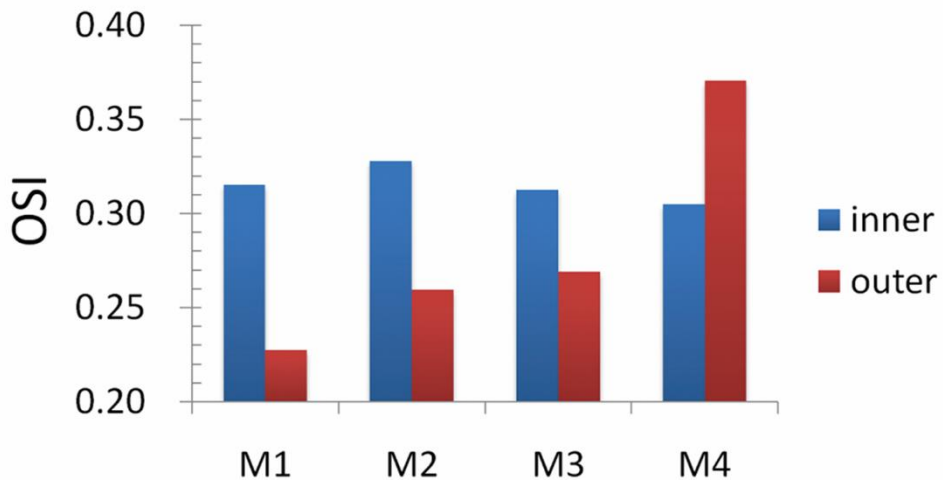


Fig. 7

Fig.7 The histogram displays oscillatory shear index (OSI) average value of the inner (the blue color column) and outer (the red color column) in each model.

## Discussion

This study constructed four numerical model with different diameters of AAo using one BAV patient's MRI images, to investigated how the hemodynamic environments of AAo will vary under the same boundary conditions. It revealed that BAV patients with vascular dilatation have altered hemodynamic environments, especially with diameter of 5.5cm.Compared to the other models, M4 has shifted higher velocity region to outer region, increased areas of high pressure and low WSS in AAo, resulting in the higher OSI in outer which overtakes inner first.

The shifted velocity region represents the eccentric flow jet directed toward the wall of the proximal AAo, and the local pressure induced by turbulence of blood flow, which is an important determinant of vascular enlargement, aneurysm growth. In a study on aortic aneurysm, it found rupture occurred in regions of predicted flow recirculation where low WSS and thrombus deposition predominated, rather regions where have high pressure and WSS<sup>14</sup>. In this study, more low WSS areas can be showed in M4 in Fig.6(t=0.17s),we could guess that M4 are much more dangerous than the others. Meanwhile, elevated OSI levels are accompanied by low WSS serve as indicators for vascular injury together.

These results indicate the AAo with diameter of 5.5cm becomes more unstable, and the step-wise influence is more remarkable when compared 5.0cm to 5.5cm with 4.0cm to 4.5cm or 4.5cm to 5.0cm. The findings support the recent guideline by AHA/ACC<sup>6</sup>, which recommended the intervention to replace the aorta when its diameter >5.5cm, even if the BAV patients are asymptomatic. And in the real patients, the hemodynamic environments of AAo could be worse, because these hemodynamic parameters alternations are likely to lead to consecutive aortic wall remodeling, which gradually results in the expansion of the arterial vessels, and make the aorta wall thinner,

the wall tension increased and vascular stiffness and elasticity decreased, which means the opportunity of aortic adverse events (dissection, rupture, or death) increases <sup>15,16,17</sup>.

Although novel indexes like ascending aortic length was developed to aid risk stratification <sup>18</sup>, the diameter is still the important index to guide operative repair, which is widely accepted worldwide. But as for patients with AAo diameter exceed 4.0cm , who are not meet the guideline recommendation to surgery, we suggest extra computational simulation to monitor abnormal hemodynamic environments could be helpful.

While it must be mentioned that, the findings of the present study are limited by some of the assumptions involves. The original computational model was carried out using original data derived from only one representative patient with BAV and aortic aneurysm. But the boundary conditions and descending aorta are fixed, effect on diameter of AAo can be studied exclusively. Future studies can enlarge the sample size, and add BAV valve classification for comparative analysis. Another limitation is that the blood vessel elasticity, the wall motion and fluid-solid interaction were not involved in all the simulations in this study. In comparison with the simulation involving structure part, this assumption may affect the accuracy of the results slightly, but it is acceptable.

## Conclusion

This study focuses on hemodynamic of BAV models with different AAo diameter levels by numerical simulation. BAV patients with vascular dilatation have altered flow patterns, pressure difference, WSS and OSI distribution features, and more parts of aorta would be affected with the increasing AAo diameters. According to the results of the numerical simulation, when AAo diameter exceeds 5.5cm, hemodynamic abnormality is more obvious with higher risk of rupture and it should be considered to replace dilated AAo. Therefore, more attention should be paid to patients with BAV.

In patients with BAV and AAo dilatation, we could use CFD numerical simulation to make an assessment and find the hemodynamics in patients with abnormal point to predict disease progression timely. This could provide hemodynamic basis for surgery

in the future. It will help to study the disease mechanism, timing of surgery, and determination of surgical options.

### **List of Abbreviations**

BAV, bicuspid aortic valve; AAo, the ascending aortic; CFD, computational fluid dynamics; WSS, wall shear stress; OSI, oscillatory shear index; CAD, computer aided design; TAWSS, time-averaged wall shear stress

### **Declarations**

Ethics approval and consent to participate

Written informed consent was obtained from the subject for the publication of this study and any accompanying, in accordance with the regulations of the local ethics committee (2016047X, Beijing Anzhen Hospital, Capital Medical University).

### **Consent for publication**

Consent for publication was obtained for the patient's data included in the study.

### **Availability of data and materials**

The datasets used and analyzed during the current study are available from the corresponding author on reasonable request, and most data generated or analyzed during this study are included in this published article and its supplementary information files.

### **Competing interests**

The authors declare that they have no competing interests.

### **Funding**

This work was supported by the Research and demonstration application of clinical diagnosis and treatment technology from Beijing Municipal Science and Commission (Z19110700660000) . National Science Foundation of China (81970393) and the National Key Technology R&D Program (No. 2015BAI12B03), and Beijing Major Science and Technology Projects from Beijing Municipal Science and Technology Commission(Z171100001017083).

### **Author contributions**

T.Z. and S.Z. researched data and participated in writing of the manuscript. J.M.Z. performed the experiments, J.F.O. and S.J.L. contributed to the discussion. T.Z., J.M.Z. provided oversight for the project and participated in editing of the manuscript.

### **Acknowledgements**

The authors appreciate Anqiang Sun(Ph.D. & Associate Professor) and Minjia Zhu (M.S.) who are members of the Key Laboratory for Biomechanics and Mechanobiology of Ministry of Education, School of Biological Science and Medical Engineering, Beihang University.

## Reference

1. Bravo-Jaimes K, Prakash SK. Genetics in bicuspid aortic valve disease: Where are we?. *Prog Cardiovasc Dis.* 2020;63(4):398-406. doi:10.1016/j.pcad.2020.06.005
2. Siu SC, Silversides CK. Bicuspid aortic valve disease. *J Am Coll Cardiol.* 2010;55(25):2789-800.
3. Rodríguez-Palomares JF, Dux-Santoy L, Guala A, et al. Aortic flow patterns and wall shear stress maps by 4D-flow cardiovascular magnetic resonance in the assessment of aortic dilatation in bicuspid aortic valve disease. *J Cardiovasc Magn Reson.* 2018;20(1):28. doi:10.1186/s12968-018-0451-1
4. Bonomi D, Vergara C, Faggiano E, Stevanella M, Conti C, Redaelli A, et al. Influence of the aortic valve leaflets on the fluid-dynamics in aorta in presence of a normally functioning bicuspid valve. *Biomech Model Mechanobiol.* 2015;14(6):1349-61.
5. Meierhofer C, Schneider EP, Lyko C, Hutter A, Martinoff S, Markl M, et al. Wall shear stress and flow patterns in the ascending aorta in patients with bicuspid aortic valves differ significantly from tricuspid aortic valves: a prospective study. *Eur Heart J Cardiovasc Imaging.* 2013;14(8):797-804.
6. Otto CM, Nishimura RA, Bonow RO, Carabello BA, Erwin JP 3rd, Gentile F, Jneid H, Krieger EV, Mack M, McLeod C, O'Gara PT, Rigolin VH, Sundt TM 3rd, Thompson A, Toly C. 2020 ACC/AHA Guideline for the Management of Patients With Valvular Heart Disease: Executive Summary: A Report of the American College of Cardiology/American Heart Association Joint Committee on Clinical Practice Guidelines. *Circulation.* 2021 Feb 2;143(5):e35-e71.
7. Hahn RT, Roman MJ, Mogtader AH, Devereux RB. Association of aortic dilation with regurgitant, stenotic and functionally normal bicuspid aortic valves. *Journal of the American College of Cardiology.* 1992;19(2):283-8.
8. Michelena HI, Khanna AD, Mahoney D, Margaryan E, Topilsky Y, Suri RM, et al. Incidence of aortic complications in patients with bicuspid aortic valves. *JAMA.* 2011;306(10):1104-12.
9. Poinsot TJ, Lelef SK. Boundary conditions for direct simulations of compressible viscous flows. *Journal of Computational Physics.* 1992;101(1):104-29.
10. Taylor CA, Hughes TJ, Zarins CK. Finite element modeling of three-dimensional pulsatile flow in the abdominal aorta: relevance to atherosclerosis. *Ann Biomed Eng.* 1998;26(6):975-87.
11. Feintuch A, Ruengsakulrach P, Lin A, Zhang J, Zhou YQ, Bishop J, et al. Hemodynamics in the mouse aortic arch as assessed by MRI, ultrasound, and numerical modeling. *Am J Physiol Heart Circ Physiol.* 2007;292(2):H884-92.
12. van der Giessen AG, Groen HC, Doriot PA, de Feyter PJ, van der Steen AF, van de Vosse FN, et al. The influence of boundary conditions on wall shear stress distribution in patients specific coronary trees. *J Biomech.* 2011;44(6):1089-95.

13. Barker AJ, Markl M, Burk J, Lorenz R, Bock J, Bauer S, et al. Bicuspid aortic valve is associated with altered wall shear stress in the ascending aorta. *Circ Cardiovasc Imaging*. 2012;5(4):457-66.
14. Boyd AJ, Kuhn DC, Lozowy RJ, Kulbisky GP. Low wall shear stress predominates at sites of abdominal aortic aneurysm rupture. *J Vasc Surg*. 2016;63(6):1613-1619. doi:10.1016/j.jvs.2015.01.040
15. Nkomo VT, Enriquez-Sarano M, Ammash NM, Melton LJ, 3rd, Bailey KR, Desjardins V, et al. Bicuspid aortic valve associated with aortic dilatation: a community-based study. *Arterioscler Thromb Vasc Biol*. 2003;23(2):351-6.
16. Tadros TM, Klein MD, Shapira OM. Ascending aortic dilatation associated with bicuspid aortic valve: pathophysiology, molecular biology, and clinical implications. *Circulation*. 2009;119(6):880-90.
17. den Reijer PM, Sallee D, 3rd, van der Velden P, Zaaijer ER, Parks WJ, Ramamurthy S, et al. Hemodynamic predictors of aortic dilatation in bicuspid aortic valve by velocity-encoded cardiovascular magnetic resonance. *J Cardiovasc Magn Reson*. 2010;12:4.
18. Wu J, Zafar MA, Li Y, et al. Ascending Aortic Length and Risk of Aortic Adverse Events: The Neglected Dimension. *J Am Coll Cardiol*. 2019;74(15):1883-1894. doi:10.1016/j.jacc.2019.07.078

# Supplementary Files

This is a list of supplementary files associated with this preprint. Click to download.

- [renamed393f6.mp4](#)
- [renamed5e5b7.mp4](#)
- [renamed6d10b.mp4](#)
- [renamed8f6ae.mp4](#)
- [renamed9267a.mp4](#)
- [renameda3993.mp4](#)
- [renameda3f4b.mp4](#)
- [renameda79e4.mp4](#)
- [renameda8345.mp4](#)
- [renameddbf4d.mp4](#)
- [renamede41e1.mp4](#)
- [renamedefe5c.mp4](#)